

Research on Collaborative Solution for Enhancing the Resilience of All DC Wind Farms Against Bipolar Short-Circuit Faults

Kunyu Hong¹, Haiyun Wang^{1*}, Junlong Lu², Huan Wang², Yibo Wang²

1 College of Electrical Engineering, Xinjiang University, Urumqi 830047, China;

2 Institute of Electrical Engineering, Chinese Academy of Science, Beijing 100190, China;

(*Haiyun Wang: 327028229@qq.com)

ABSTRACT

The inherent vulnerability of medium-voltage DC (MVDC) collection systems in all-DC wind farms to bipolar short-circuit faults represents a significant barrier to widespread adoption. Such faults induce uncontrolled over-currents, voltage collapse, and potential grid disconnection. Consequently, enhancing fault ride-through capability is critical for ensuring wind farm resilience. This paper proposes an integrated resilience enhancement scheme combining adaptive topology reconfiguration with grid-forming control. The fault evolution dynamics are first analyzed within representative MVDC wind farm architectures. An innovative solution is then introduced, incorporating a medium-voltage bus current-limiting module and an energy-storage capacitor compensation unit, which jointly enable rapid fault isolation and provide energy support. Furthermore, a three-tier coordinated response mechanism leverages the active power support capabilities of grid-side converters. Comprehensive simulation studies validate that the proposed integrated approach effectively mitigates the destructive effects of short-circuit faults, concurrently enhancing the system's autonomous voltage recovery capability and significantly improving the efficiency of post-fault resilient power recovery.

Keywords: onshore wind integration systems, pole-to-pole fault ride-through, system resilience, grid-forming control, transient overcurrent suppression

1. INTRODUCTION

Wind power, recognized as one of the most mature and technologically advanced methods of power generation among renewable energy sources, has experienced rapid development in recent years. By the end of June 2024, China's cumulative grid-connected wind power capacity had reached 467 GW, with onshore

wind power accounting for over 90% of this total [1]. Furthermore, China's "Renewable Energy Development Plan for the 14th Five-Year Plan" explicitly mandates the concurrent development of centralized and distributed generation systems, with a focus on vigorously promoting large-scale wind and photovoltaic base projects in desert, Gobi, and desertified regions [2].

However, conventional wind power transmission systems that employ "AC Collection - AC Transmission" and flexible HVDC systems that use "AC Collection - DC Transmission" inevitably encounter significant challenges, including excessive reactive charging currents and overvoltage issues caused by AC cables. In contrast, DC-based wind power systems built with DC wind turbines and featuring "DC Collection - DC Transmission" offer distinct advantages. These systems not only mitigate the reactive charging current and overvoltage problems associated with AC cables but also exhibit reduced power losses. Consequently, such DC-based wind power systems have become a major research focus in both industry and academia [3-6].

In this field, DC-based wind power generation systems can be divided into two main topologies according to their energy collection methods: parallel configurations and series configurations [7-8]. In the parallel network setup, high-ratio step-up voltage conversion takes place directly at the output terminals of the DC wind turbines. This method substantially lowers step-up losses and cuts down on energy losses in the power collection process. Moreover, by using turbine-side DC-DC step-up converters, independent control of turbine-side voltage and power becomes possible. As a result, this parallel configuration stands out as the preferred topology for DC-collection wind farms.

Coordinated switching among multiple control strategies plays a key role in achieving efficient and stable operation in DC-collection-based wind farms. Its main benefit comes from adapting dynamically to

complex operating conditions and optimizing re-source allocation [9-10]. Key grid-forming control methods include droop control and virtual synchronous generator control. Virtual synchronous generator control serves as a voltage and frequency regulation strategy that mimics the dynamic traits of synchronous generators. This method equips power electronic devices, like modular multilevel converters, with frequency and voltage regulation abilities similar to those of traditional synchronous machines. For example, by switching coordinately between virtual inertia control and droop control, the system can quickly handle wind speed changes or grid frequency drops [11-13]. In fault situations, coordinated SVG-DFIG control that combines zero DC voltage control with power-limiting strategies effectively curbs current surges and keeps voltage stable [14-16]. When it comes to optimizing power distribution, wake steering through active pitch control [17-19], paired with coordinated rotor control, can boost overall farm output by more than 10% and cut structural loads at the same time [20]. This combined approach goes beyond the drawbacks of single-strategy controls, striking a balance among dynamic response, operational backup, and cost-effectiveness.

Research into fault ride-through schemes for medium-voltage DC collection lines re-mains underexplored in the current literature. [21] suggests an improved modular clamp T-type MMC topology with fault-blocking capability and energy dissipation features. However, this topology has built-in structural complexity, ramping up challenges in design, commissioning, and maintenance. [22] presents an unbalanced power absorption strategy drawing on converter station power margins, along with a coordinated control approach between the converter station and the braking resistor. Still, this study skimps on deeper looks at how wind farm load shedding, converter station power transfer, and DBR operation interact coordinately. [23] puts forward a coordinated control strategy using a hybrid modular multilevel converter with half-bridge and full-bridge submodules. By managing DC voltage to hold back fault current, this strategy pulls off fault ride-through without blocking the converter. The work shows real innovation, and simulations back up its effectiveness. But it overlooks solid thought on real engineering hardware limits and wind farm internal dynamics. [24] examines bipolar short-circuit features in a photovoltaic medium-voltage DC collection system, suggesting an active overvoltage suppression method, which lays a theoretical groundwork for system protection design. Even so, the

suggested overvoltage suppression method puts tough demands on PV mod-ules, curbing its usefulness. [25] tackles high-voltage DC transformers in all-DC offshore wind farms, offering a hybrid modular topology. It looks at commutation failure fault traits and suggests a matching FRT strategy. However, the study doesn't properly cover long-term stability, real hardware limits, or the vital matter of energy balance in unfaulted phases.

To tackle these issues, this paper centers on creating a fault ride-through control method for DC-collection-based wind farms that rely on permanent magnet synchronous generator wind turbines as the main power source. The study starts by examining the system topology and control setup. Next, aiming at pole-to-pole short-circuit faults in the medium-voltage DC collection and export lines, we suggest an integrated FRT control approach that blends topology improvements with coordinated control strategies. This method makes sure that when a fault hits, the faulty branch gets isolated quickly while keeping the non-faulty branches running smoothly, which leads to effective fault ride-through and keeps the system stable. The scheme's effectiveness gets thoroughly checked through MATLAB/Simulink simulations.

2. TOPOLOGY AND CONTROL APPROACHES FOR DC-COLLECTION WIND FARMS

2.1 Topological Configuration of DC-Collection Wind Farms

The designed DC-collection wind farm topology sidesteps voltage synchronization and harmonic problems common in AC collection systems. It cuts down on the number of needed grid-side converters, boosting economic feasibility, as shown in Figure 1. Each of the multiple branches includes a DC wind turbine (DCWT) that outputs low-voltage DC. This gets stepped up to medium-voltage DC using DC/DC converters. Outputs from all branches connect in parallel to create a medium-voltage DC collection line, which sends power to the grid-side modular multilevel converter station for inversion and grid tie-in.

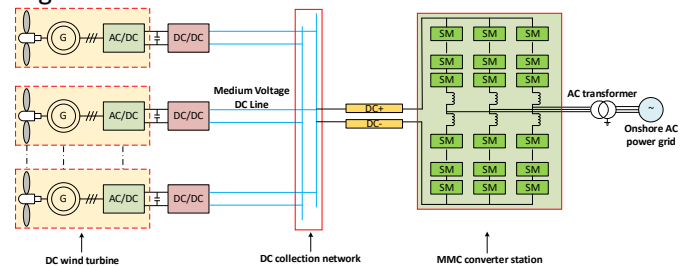


Fig. 1 Topology structure of DC-integrated aggregation for wind farms

the short-circuit path, further increasing the fault current until either energy depletion or protection operation occurs. This energy release process is governed by an RL circuit:

$$L_{eq} \frac{di}{dt} + R_{eq} i = 0 \quad (5)$$

Where the equivalent capacitance $L_{eq} = L_{dc} + L$, L_{dc} for the converter station leveling wave reactor; R_{eq} denotes the continuity circuit resistance. The solution is:

$$i(t) = I_0 e^{-\frac{R_{eq} t}{L_{eq}}} \quad (6)$$

3.2 Topological Modifications for Enhanced Fault Ride-Through (FRT) Capability

As analyzed previously, during a fault occurrence, the affected feeder must be shut down and disconnected. However, the wind turbines on the faulted feeder continue generating electrical power and feeding it toward the grid side. Therefore, an energy-dissipating blocking device must be incorporated on the wind turbine side, as illustrated in Figure 4.

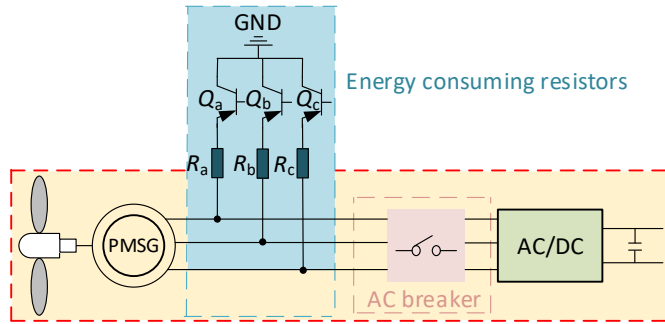


Fig. 4 Energy dissipation blocking device

In the steady-state operation of the system, the energy-consuming parts Q_a , Q_b , Q_c remain in the blocking state, with no energy consumed through the resistors R_a , R_b , R_c ; the circuit breaker stays closed, allowing electrical energy to be transmitted from the wind turbine to the power grid. When a short-circuit fault occurs between the poles of the line, the AC circuit breaker opens, Q_a , Q_b , Q_c conduct, redirecting the power generated by the wind turbine to R_a , R_b , R_c for conversion into thermal energy; simultaneously, a shutdown signal is sent to the wind turbine, thereby blocking the continuation of the fault current, protecting other system equipment from damage, and completing the shutdown and isolation operation.

The aforementioned analysis indicates that short-circuit faults in the converging line, occurring between the poles, directly cause the associated capacitor voltage to exhibit a significant transient drop. When the inter-pole voltage falls to the protection threshold, the current blocking module is promptly activated to establish a fault

current blocking path, thereby preventing capacitor discharge to the short-circuit point. The current blocking module, as shown in Figure 5, suppresses the rate of capacitor voltage decline and the rise of short-circuit current.

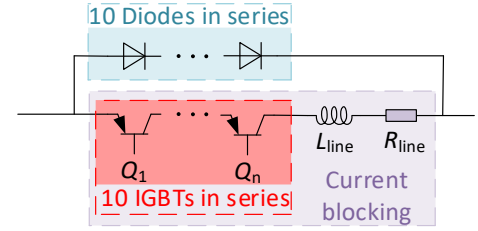


Fig. 5 Current blocking module

Several insulated gate bipolar transistors (IGBTs) and diodes are connected in antiparallel, with a current-limiting inductor L_{line} and current-limiting resistor R_{line} connected in series; in the event of a system fault, the reverse diode in Figure 5 creates a clamping effect on the discharge path, forcing capacitive energy to discharge solely through the IGBT branch that includes the current-limiting inductor and resistor. The current-limiting resistor in the IGBT branch achieves the effect of effectively reducing the rate and peak value of capacitive discharge in the faulty branch. Since the voltage withstand level of a single IGBT can reach up to 6.5kV, ten IGBTs (Q_1 , Q_2 , ..., Q_{10}) are connected in series within the IGBT branch to meet the requirements for dynamic voltage equalization.

Additionally, to mitigate the magnitude of voltage sag and expedite operational recovery of unaffected branches post-fault, a voltage-supporting compensation branch is integrated across capacitors on each collection line. This branch employs an IGBT (Q_s) configured in antiparallel with a diode, as depicted in Figure 6. During steady-state operation, Q_s remains continuously conducting to facilitate pre-charging of the compensation capacitor C_s . Upon completion of the charging process, Q_s transitions to the off-state. When a short-circuit fault occurs, the current-blocking module concurrently transmits a gate pulse to Q_s during its activation, thereby integrating the compensation branch into the main circuit. This action establishes a parallel capacitive network between C_s and the medium-voltage modular capacitor C . The composite capacitance topology effectively suppresses transient bus voltage sags through dynamic reactive power compensation. Following fault clearance, the compensation branch is automatically de-energized via the central logic control unit.

During the fault traversal process, the DC/DC converter does not require blocking operation, as it utilizes the remaining energy from its outlet capacitor

and the compensating capacitor charge to collectively supply energy to the LV side and minimize the amplitude of DC voltage fluctuations at the machine-side converter output. After the fault is cleared, the capacitor recharging process can be shortened because the module capacitor charge on the MV side has not been fully discharged through the fault point, and the capacitor compensation branch has been actively withdrawn from operation.

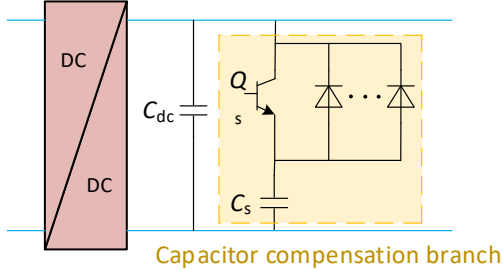


Fig. 6 Capacitor compensation branch

3.3 Calculation of System Design Parameters

Based on the analysis of operational timing characteristics in the relay protection system, the system can complete the detection and transmission of fault characteristic signals within a 4 ms time window after fault inception. This ensures the synchronous activation of the current blocking module and the capacitor compensation branch. During fault occurrence, to effectively suppress transient fluctuations in the machine-side converter output DC voltage, the dip amplitude of the MV-side capacitor voltage must be strictly limited to within 10% of the rated value before the fault current blocking action is executed. The resulting total loop inductance satisfies:

$$L_{line} + L_s > 11.7 \text{ mH} \quad (7)$$

Where L_s is the medium-voltage DC line inductance (valued at 2.5mH in this study), the current-limiting inductance in the current blocking module should thus be:

$$L_{line} > 9.2 \text{ mH} \quad (8)$$

Additionally, to eliminate the loop current generated within the current blocking module upon activation and to account for power loss on the resistor, the value of the current-limiting resistor R_{line} should not be excessively large; in this paper, it is set at 2.3Ω .

In the fault ride-through control method proposed in this study, the transient drop in bus voltage is suppressed through the synergistic action of the medium-voltage side capacitor and the compensation capacitor. The energy retention level of the capacitor voltage during fault ride-through is directly related to the system voltage stability margin and the energy recovery

efficiency of the medium-voltage capacitor after fault clearance, constituting a key constraint—namely, that the capacitor voltage drop during fault ride-through should not exceed 10%. According to the principle of energy conservation, the value of the compensation capacitor should satisfy:

$$\frac{1}{2} C_{total} (U_N^2 - U_f^2) \geq P_{load} \cdot t_f \quad (9)$$

$$\begin{cases} C_{total} = C_{dc} + C_s \\ U_f = U_N - \Delta U \end{cases} \quad (10)$$

Where C_{total} is the sum of medium-voltage side capacitance C_{dc} and compensation capacitance C_s ; U_N is the rated voltage of medium-voltage DC bus; ΔU is the drop in capacitor voltage during the fault; P_{load} is the equivalent load power of the system; and t_f is the fault duration. Considering a certain margin, the compensation capacitor C_s should be selected as 8 mF.

4. DESIGN OF A MULTI-LEVEL COORDINATED CONTROL STRATEGY

4.1 Control Strategy Design for Grid-Side Converters

In DC collection wind farms under fault conditions, the control strategy for grid-side converters is critical to maintain stable operation. The propagation paths of fault currents within the GSC are illustrated in Figure 7.

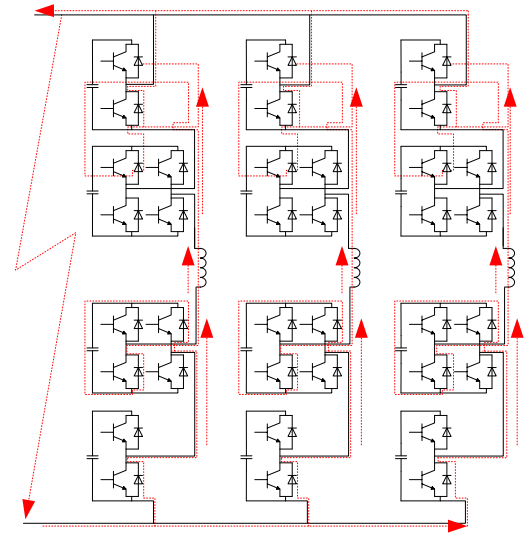


Fig. 7 Flow path of fault current in grid-side converters

To endow the grid-side converter with characteristics analogous to those of a conventional synchronous generator, a virtual synchronous generator (VSG) control strategy is introduced. The VSG emulates the rotor swing equation and droop characteristics of traditional synchronous generators, enabling the converter to respond to grid frequency and voltage

variations. Consequently, it provides inertia emulation and frequency regulation capabilities.

The control structure depicted in Figure 8 empowers the grid-side converter with voltage and frequency support capabilities. Leveraging the inherent topological characteristics of the modular multilevel converter (MMC), this structure integrates the electromechanical transient model of the virtual synchronous generator. Grid active support functionality is realized through hierarchical control, implemented as follows:

1) Voltage Support Control. In the outer voltage control loop, an excitation control principle emulating synchronous generators is implemented, establishing the reactive power-voltage droop equation:

$$Q_{ref} = Q_{set} + K_Q(V_{ref} - V_{pcc}) \quad (11)$$

Where K_Q is the reactive power modulation coefficient, V_{ref} is the reference voltage, and V_{pcc} is the grid point voltage. Through real-time acquisition of grid voltage signals, the modulating voltage amplitude of the MMC submodule is adjusted to dynamically compensate for grid reactive power deficit and suppress voltage fluctuations. This strategy can simulate the autonomous voltage regulation characteristics of synchronous machines, making it especially suitable for voltage stabilization requirements.

2) Frequency Support Control. The frequency control loop implements the virtual synchronous generator rotor swing equation:

$$J \frac{d\Delta\omega}{dt} = P_{ref} - P_{out} - D_p \Delta\omega \quad (12)$$

Where J is the virtual inertia, D_p is the damping coefficient, and $\Delta\omega$ is the frequency deviation. This module dynamically adjusts the active power output of the MMC by simulating the mechanical inertia response and converting the power deviation into a frequency adjustment signal, thereby achieving inertia response and primary frequency adjustment. Compared to traditional droop control, the inertia characteristic of the VSG can delay the frequency change rate, while the damping coefficient suppresses frequency oscillations, thereby enhancing system transient stability.

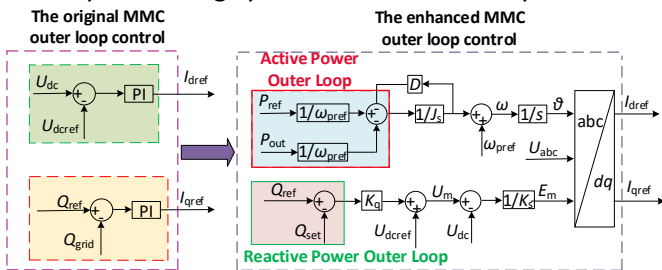


Fig. 8 Enhanced control block diagram for the outer loop of the grid-side converter

4.2 Design of Multi-Criteria Decision Control Strategy

From the previous analysis, the faulty branch must be shut down and isolated during fault occurrence, with this paper opting to achieve the shutdown operation through pitch angle control. During steady-state operation of the system, it operates in maximum power tracking mode, with the pitch angle maintained at 0° . When a fault occurs on the line, the wind turbine exits MPPT mode, during which the pitch angle increases to a specific angle ϑ_s , causing the fan blades to gradually stop rotating and completing the shutdown operation for the turbine on the faulty line.

Figure 9 illustrates the switching process between normal operation mode and fault state mode. Taking three branches as an example, I_{line1} , I_{line2} and I_{line3} represent the currents in three parallel branches; these are compared to determine if their values are equal—if so, the logic gate in the upper part of the figure outputs a logic signal of 1; otherwise, it outputs 0. Simultaneously, the differences between the three currents are checked against a set error range: when a fault occurs in one branch, the currents in the other two will be smaller than in the faulty branch, prompting the logic gate in the lower part of the figure to output a logic signal of 1; otherwise, it outputs 0. This output is then connected to an "OR" logic gate, followed by a memory module, ensuring the output remains at 1 as long as a fault persists in the branch. Connecting this output to the "OR" logic gate, followed by the memory module, ensures that the output remains at 1 as long as a fault occurs on the branch. The output of the memory module serves as the final hold state signal. Finally, a switch module determines the final output value: its control terminal connects to the "AND" logic gate in the upper part of the diagram, outputting 0 during steady-state operation; otherwise, it indicates a fault state and outputs the logic signal 1 from the memory module, at which point the pitch angle begins to increase, and the system exits MPPT mode until shutdown.

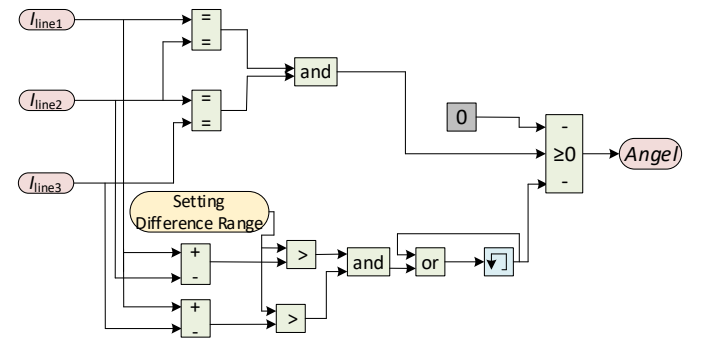


Fig. 9 Logic diagram for multi-condition decision-making-based control signal generation

The aforementioned analysis indicates that short-circuit faults in the pooling line between the poles directly cause the associated capacitor voltage to exhibit a significant transient drop, accompanied by the formation of a substantial short-circuit current. These serve as the fault judgment criteria: when the capacitor voltage falls below the set threshold and the current exceeds its threshold, the system transitions from normal to fault state, generating a trigger signal simultaneously. At this point, the IGBTs mentioned in Section 3.2 conduct or block according to the specified logic, preventing capacitor discharge to the short-circuit point to slow the decline in capacitor voltage and suppress the rise in short-circuit current.

5. DISCUSSION

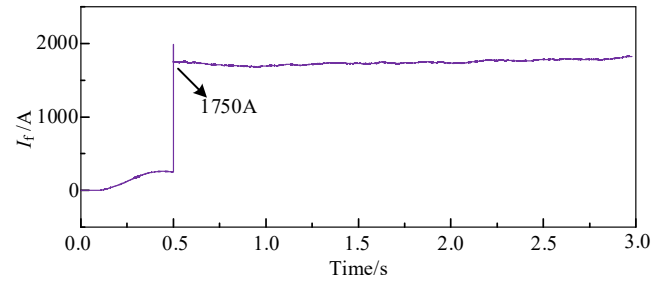
To verify the control strategy for the DC converging wind farm proposed in this paper, along with the effectiveness of the fault ride-through control method, a simulation model as shown in Figure 1 was constructed using MATLAB/Simulink software; the relevant system simulation parameters are presented in Table 1.

Table 1. Main simulation parameters of the system

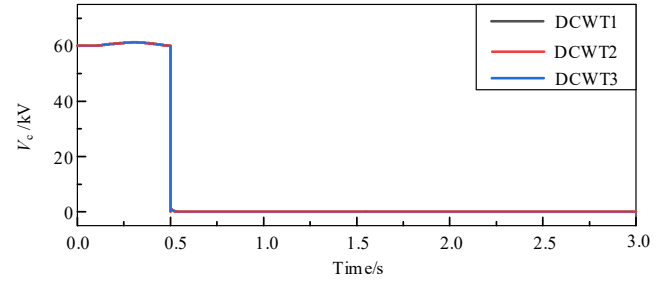
Simulation parameters	Value
Rated capacity of wind farm/MVA	15
System frequency/Hz	50
Outlet voltage of MSC/V	1050
Outlet voltage of DC/DC converter/kV	± 30
Number of bridge arm sub-modules/pc	60
FBSM percentage/%	50
RMS value of grid-side line voltage/kV	35

In the simulation, the wind farm output power is set to 15 MW, with an inter-pole short-circuit fault occurring at 0.5 s on the MV DC converging line of a wind turbine.

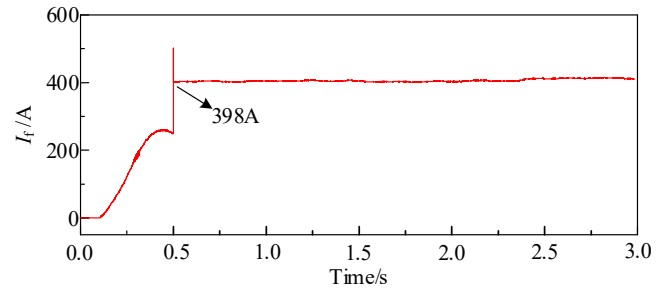
Figure 10a,10b depicts the simulation waveforms of the current and voltage on the branch line when the fault occurs without any protective measures. From the simulation results, it is evident that upon the instantaneous occurrence of the inter-pole short-circuit fault, the stored energy in the capacitor on the MV side is rapidly released through the short-circuit path, causing the capacitor voltage to drop sharply while simultaneously generating a very high short-circuit current; once the capacitor voltage falls to 0, it ceases to discharge, and the energy stored in the branch inductance is released into the short-circuit loop, forming a sustained fault current until the energy is depleted or protective action is initiated.



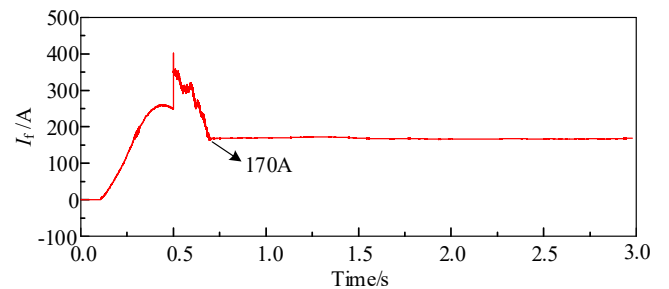
(a) Branch current under no mitigation measures applied



(b) Branch voltage under no mitigation measures applied



(c) Fault current with only the current-blocking module engaged



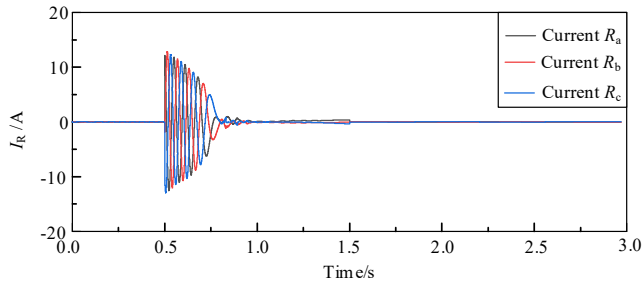
(d) Fault current under the implementation of fault ride-through control strategy

Fig. 11 Fault condition line current and inter pole voltage

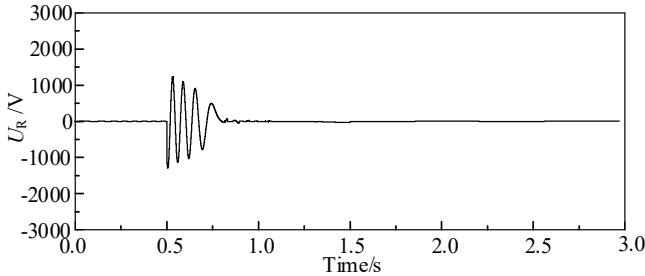
Figure 11(c) illustrates the branch current when only the current-blocking module is employed, revealing that the short-circuit inrush current is significantly suppressed, as evident from the waveform. In Figure 11(d), with the current-blocking module engaged alongside the synchronized integration of the capacitor compensation branch—and following the fault ride-through control method after removing the faulty unit—the branch current is shown, indicating further

suppression of the short-circuit inrush current, which remains within the maximum tolerance of the system components.

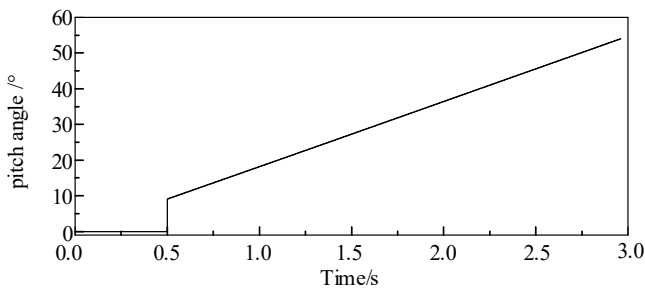
As indicated by the prior analysis, the turbine in the faulty branch continues to generate and transmit power to the grid during the fault period, whereas it should be shut down and isolated in accordance with the fault ride-through control method. Figure 15 depicts the effects of the fault ride-through control method on the turbine side following the fault occurrence. Initially, the energy-consuming blocking device and the machine-side AC circuit breaker are activated, directing all power generated by the turbine to R_a , R_b , and R_c , where it is converted into thermal energy and dissipated. Figures 12(a) and (b) display the current and resistor voltage waveforms for the energy-consuming blocking device on the turbine side, demonstrating that the turbine's generated power is progressively dissipated and ceases transmission to the grid until the faulty turbine is isolated.



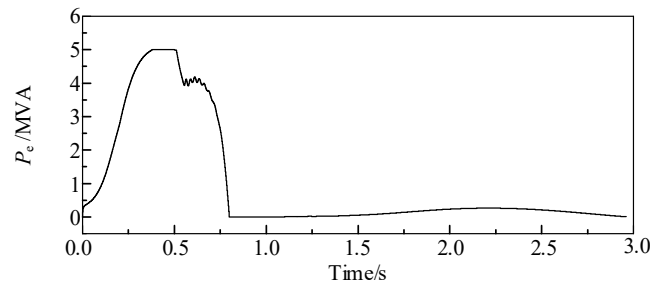
(a) Branch current through the energy dissipation blocking device



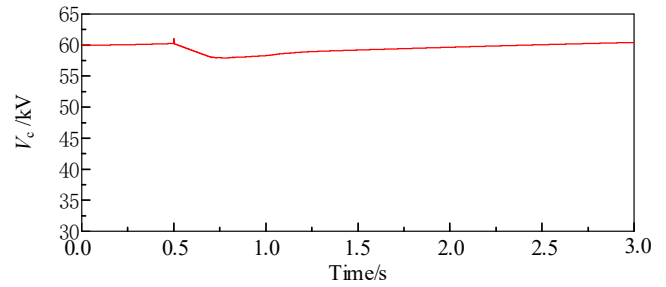
(b) Voltage across the resistor within the energy dissipation blocking device



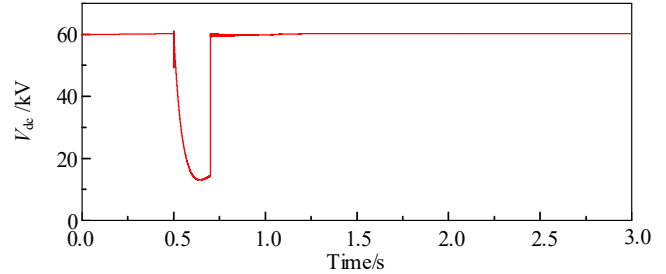
(c) Pitch angle of the wind turbine prior to disconnection



(d) Active power output of the wind turbine prior to disconnection



(e) Capacitor voltage in the non-faulted branch



(f) DC-side voltage in the non-faulted branch

Fig. 12 Application of FRT Control Method

Figures 12(c) and (d) illustrate the active power output from the turbine slated for removal and its pitch angle; as evident from these figures, under the fault ride-through control method, the pitch angle of the affected turbine gradually increases, ultimately halting power generation in the faulty branch.

Except for the branch containing the faulted WTG, the other non-faulted branches should achieve fault ride-through using the proposed control method and continue to operate stably. The capacitor voltage waveforms of the non-faulted branch, along with the DC-side voltage waveforms, are presented in Figure 12(e)(f).

6. CONCLUSIONS

In this study, an in-depth investigation has been conducted into the short-circuit fault issues associated with medium-voltage DC collection lines in DC-connected wind farms, and a fault ride-through control method is proposed that incorporates topological improvements and coordinated control strategies. The conclusions are as follows:

(1) Owing to the presence of MVDC collection lines in DC-connected wind farms, the occurrence of inter-pole short-circuit faults in a single branch affects the entire wind farm, leading to a sharp voltage drop and substantial inrush current, ultimately resulting in a power outage.

(2) To address the limitations of the existing collection line topology under fault conditions, this study proposes targeted improvement measures. The improved topology more effectively limits the fault current and reduces system voltage fluctuations during faults, thereby significantly enhancing the system's stability and reliability.

(3) Through the development of a multi-level coordinated control strategy that integrates the grid-side controller, pitch angle controller, and fault ride-through device control, along with appropriate adjustments to the parameters and action logic of each control component, the system achieves rapid response and seamless transition during faults. This approach ensures stable operation of the wind farm throughout the fault duration while minimizing the fault's impact on overall system performance.

ACKNOWLEDGEMENT

This research was funded by the National Key Research and Development Program of China, grant number 2021YFB1507000. At the same time, thanks to the support from the Institute of Electrical Engineering of the Chinese Academy of Sciences.

REFERENCE

[1] National Energy Administration. Transcript of the National Energy Administration's press conference for the first half of 2024. Available online: (accessed on 31 July 2024).

[2] Xinhua News Agency. Outline of the Fourteenth Five-Year Plan for the National Economic and Social Development of the People's Republic of China and the Vision for 2035. Available online: (accessed on 13 March 2021).

[3] Wang X, Yang M, Wen J. DR-MMC Hub Based Hybrid AC/DC Collection and HVDC Transmission System for Large-Scale Offshore Wind Farms. *Journal of Modern Power Systems and Clean Energy* 2025;13:452-461.

[4] Li B, Wang Y, Jiao Y, Zhao X, Suo Z, Li R. Bidirectional Hybrid Isolated DC Transformer for All-DC Collection and Transmission System. *IEEE Transactions on Power Electronics* 2025;40:11598-11615.

[5] Bai X, Fan Y, Hou J, Sun Y, Liu Y, Liu J. Reliability evaluation of DC gathering system in onshore wind farm

based on RBD-SMC. *Sustainable Energy* 2024;40:101549-101561.

[6] Li B, Liu J, Wang Z, Zhang S, Xu D. Modular High-Power DC-DC Converter for MVDC Renewable Energy Collection Systems. *IEEE Transactions on Industrial Electronics* 2021;68:5875-5886.

[7] Song Y, Zhang Z, Xu Z. Modular Combined DC-DC Autotransformer for Offshore Wind Power Integration with DC Collection. *Appl. Sci* 2022;12:1810.

[8] Coffey S, Timmers V, Li R, Wu G, Egea-Àlvarez A. Review of MVDC Applications, Technologies, and Future Prospects. *Energies* 2021;14:8294.

[9] Xu L, Liu C, Zhang J, Tian Z, Feng P, Huang M. Characteristics Evaluation and Coordinated Control Strategy of Power-Electronics-Based MMC-HVDC Systems Connected with Wind Farms. *Appl. Sci* 2025;15:2582.

[10] Hu P, Yin R, He Z, Wang C. A Modular Multiple DC Transformer Based DC Transmission System for PMSG Based Offshore Wind Farm Integration. *IEEE Access* 2020;8:15736-115746.

[11] Nguyen V.T, Truong T.B.T, Truong Q.V, Nguyen H.V.P, Duong M.Q. Iterative Learning Control for Virtual Inertia: Improving Frequency Stability in Renewable Energy Microgrids. *Sustainability* 2025;17:6727.

[12] Miao L, Zhou N, Ma J, Liu H, Zhao J, Wei X, Yin J. Current Status, Challenges and Future Perspectives of Operation Optimization, Power Prediction and Virtual Synchronous Generator of Microgrids: A Comprehensive Review. *Energies* 2025;18:3557.

[13] Cao X, Zhang R, Li J, Ji L, Wei X, Geng J, Li B. Analysis of Grid-Connected Damping Characteristics of Virtual Synchronous Generator and Improvement Strategies. *Electronics* 2025;14:2501.

[14] Peng Y, Wang H, Zhao Q, Nan D, Li W. Research and Application of Combined Reactive Power Compensation Device Based on SVG+SC in Wind Power Gathering Area. *Appl. Sci* 2022;12:10906.

[15] Tian X, Chi Y, Li Y, Tang H, Liu C, Su Y. Coordinated damping optimization control of sub-synchronous oscillation for DFIG and SVG. *CSEE Journal of Power and Energy Systems* 2021;7:140-149.

[16] Kang Z, Li J. Zero-Voltage Ride-Through Scheme of PMSG Wind Power System Based on NLESO and GFTSMC. *Electronics* 2023;12:4348.

[17] Thapa K.B, Jayasawal K. Pitch Control Scheme for Rapid Active Power Control of a PMSG-Based Wind Power Plant. *IEEE Transactions on Industry Applications* 2020;56:6756-6766.

[18] Tang X, Yin M, Shen C, Xu Y, Dong Z, Yun Z. Active Power Control of Wind Turbine Generators via

Coordinated Rotor Speed and Pitch Angle Regulation. IEEE Transactions on Sustainable Energy 2019;10:822-832.

[19] Luo H, Hu Z, Zhang H, Chen H. Coordinated Active Power Control Strategy for Deloaded Wind Turbines to Improve Regulation Performance in AGC. IEEE Transactions on Power Systems 2019;34:98-108.

[20] Kumar D, Shireen W, Ram N. Grid Integration of Offshore Wind Energy: A Review on Fault Ride Through Techniques for MMC-HVDC Systems. Energies 2024;17:5308.

[21] Jiang S, Xin Y, Li G, Wang L. A Novel DC Fault Ride-Through Method for Wind Farms Connected to the Grid Through Bipolar MMC-HVDC Transmission. IEEE Transactions on Power Delivery 2020;35:2937-2950.

[22] Kim C, Kim W. Low-Voltage Ride-Through Coordinated Control for PMSG Wind Turbines Using De-Loaded Operation. IEEE Access 2021;9:66599-66606.

[23] Liu Y, Jin Y, Li Z, Liu Y, Li B, Duan Z. Mechanical DC Breakers and Hybrid MMC-Based Coordinated Strategy for MMC-HVDC DC Fault Riding Through. IEEE Journal of Emerging and Selected Topics in Power Electronics 2023;11:3705-3714.

[24] Diao X, Liu F, Song Y, Xu M, Zhuang Y, Zha X. A Novel Fault Ride-Through Topology With High Efficiency and Fast Fault Clearing Capability for MVDC PV System. IEEE Transactions on Industrial Electronics 2023;70:1501-1511.

[25] Zhao P, Meng Y, Ge M, Duan Z, Wang X, Wang J. Series-Parallel Multiple Integrated Modular Multilevel DC-DC Converter for All-DC Offshore Wind Power System. IEEE Transactions on Power Delivery 2024;39:2482-2494.